2018 International Symposium on Nonlinear Theory and Its Applications,
NOLTA2018, Tarragona, Spain, September 2-6, 2018

Stability analysis of a time-delay system with quadratic nonlinearity

Griselda R. Itovich*, Franco S. Gentile†⋆ and Jorge L. Moiola‡⋆

∗ Escuela de Producción, Tecnología y Medio Ambiente, Sede Alto Valle,
Universidad Nacional de Río Negro, R8336ATG Villa Regina, Argentina
†Departamento de Matemática, Universidad Nacional del Sur, B8000CPB Bahía Blanca, Argentina
⋆ Instituto de Investigaciones en Ingeniería Eléctrica - IIIE (UNS-CONICET), B8000CPB Bahía Blanca, Argentina
‡Dpto. de Ingeniería Eléctrica y Computadoras, Universidad Nacional del Sur, B8000CPB Bahía Blanca, Argentina

Abstract—In this article, the stability of the equilibrium points of a time-delay system with quadratic nonlinearity is investigated by means of the Nyquist stability criterion. The variation of several parameters is considered, and it is found that the system exhibits infinitely many resonant Hopf-Hopf bifurcations, as well as zero-Hopf bifurcations.

1. Introduction

This work deals with the stability analysis of a nonlinear time-delay system with four parameters, including the delay. The proposed model is a generalization of a system originally presented in [1], where the authors focused on a Hopf-Hopf bifurcation with 1:2 resonance. Recent advances in the dynamics of that system were reported in [2].

The model studied in the present article includes two additional parameters, which causes the appearance of infinitely many resonant Hopf-Hopf bifurcation points.

The critical stability conditions and the appearance of Hopf bifurcations are found by a frequency-domain approach [3, 4] based on the Nyquist stability criterion [5].

2. Modified Campbell & LeBlanc's system

Consider the following system:

$$\begin{cases} \dot{x}_1 &= x_2, \\ \dot{x}_2 &= -\gamma x_1 + f(x_{1\tau}), \end{cases} \tag{1}$$

where $\gamma, \tau > 0$, $\alpha, \beta \neq 0$, $x_{1\tau} = x_1(t-\tau)$ and $f(x) = \alpha x + \beta x^2$. The previous model was studied in [1] for $\gamma = 2.5$ and $\beta = 0.9$ related with a Hopf-Hopf bifurcation with $1:2$ resonance.

To apply the graphical Hopf bifurcation theorem (GHBT) (see Theorem 6.1 in [4]) model (1) is recast as a feedback system, by defining a linear transfer function $G(s)$ and a nonlinear feedback $g(y)$ as follows:

$$G(s) = \frac{e^{-s\tau}}{s^2+\gamma}, \qquad g(y) = f(-y) = -\alpha y + \beta y^2, \tag{2}$$

where the output of the linear subsystem is $y = -x_1$. This technique was originally proposed to solve oscillations in circuits and systems [3].

The equilibrium points are found by solving $G(0)g(y^*) = -y^*$, which gives a trivial equilibrium point $y_1^* = 0$ and a nontrivial one $y_2^* = (\alpha - \gamma)/\beta$. For each equilibrium point, one can consider a linearization given by:

$$J_1 := \left.\frac{dg}{dy}\right|_{y_1^*} = -\alpha, \qquad J_2 := \left.\frac{dg}{dy}\right|_{y_2^*} = \alpha - 2\gamma. \tag{3}$$

In what follows, the stability of each equilibrium point will be studied by means of the Nyquist stability criterion (see [5]).

3. Stability of equilibrium points

3.1. Trivial equilibrium point

The characteristic function (see [3, 4]) for the equilibrium point $y_1^* = 0$ is defined as

$$\lambda_1(s) = G(s)J_1 = -\frac{\alpha e^{-s\tau}}{s^2+\gamma}. \tag{4}$$

The critical stability condition in the frequency-domain is given by $\lambda_1(i\omega) = -1$, which, from (4), can be written as $G(i\omega) = 1/\alpha$. Thus, it is convenient to study the Nyquist diagram of $G(s)$ and to determine the number of turns around the critical point $1/\alpha$.

The poles of $G(s)$ lie on the imaginary axis, at points $\pm i\sqrt{\gamma}$. The Nyquist contour should be modified in order to avoid them, including a semi-circumference of radius $\epsilon \ll 1$, as shown in Fig. 1. Consider a parametrization of the Nyquist contour. It is enough to compute its image only for positive frequencies.

For the sake of simplicity, in a first instance assume $\tau = \pi$. Later, the stability results for general values of τ will be deduced. Then each portion of the Nyquist curve will be analyzed.

(a) $s = i\omega$, $0 < \omega < \sqrt{\gamma}$. From (2), with $\tau = \pi$, it follows that

$$|G| = \frac{1}{\gamma - \omega^2}, \quad \arg(G) = -\omega\pi.$$

With $\omega = 0$, one has $\arg(G) = 0$, and the image starts on the positive real axis, at the point $1/\gamma$. As ω increases, the modulus grows, and when $\omega \to \sqrt{\gamma}$, the phase approaches $-\sqrt{\gamma}\pi$ and $|G| \to \infty$. Thus, conforming $\omega \to \sqrt{\gamma}$, there is an asymptote on the ray $\arg(\cdot) = -\sqrt{\gamma}\,\pi$.

(b) $s = \sqrt{\gamma}\, i + \epsilon e^{i\theta}$, $-\pi/2 \le \theta \le \pi/2$, with $\epsilon \ll 1$. Then

$$G(s) = \frac{\exp[-\pi(\sqrt{\gamma}\, i + \epsilon e^{i\theta})]}{(\sqrt{\gamma}\, i + \epsilon e^{i\theta})^2 + \gamma} \simeq \frac{\exp[-\pi(\sqrt{\gamma}\, i + \epsilon e^{i\theta})]}{2\epsilon i \sqrt{\gamma} e^{i\theta}}$$
$$= \frac{\exp[-\pi(\sqrt{\gamma}\, i + \epsilon e^{i\theta}) - i(\theta + \pi/2)]}{2\sqrt{\gamma}\epsilon}, \tag{5}$$

and it follows that $|G| = e^{-\epsilon\pi\cos\theta}/(2\sqrt{\gamma}\epsilon)$ and

$$\arg(G) = -\pi\sqrt{\gamma} - \epsilon\pi\sin\theta - \theta - \pi/2 \simeq -\pi\sqrt{\gamma} - \theta - \pi/2.$$

Thus, as θ varies between $-\pi/2$ and $\pi/2$, $\arg(G)$ varies from $-\sqrt{\gamma}\pi$ to $-(\sqrt{\gamma}+1)\pi$, respectively.

(c) $s = i\omega$, $\sqrt{\gamma} < \omega < \infty$. In this case $|G| = 1/(\omega^2 - \gamma)$, $\arg(G) = (1-\omega)\pi$, and the phase decreases linearly as ω increases, so that the image describes infinitely many turns around the origin of the $G-$plane in the clockwise sense, while $|G|$ decreases. As $\omega \to \sqrt{\gamma}^+$, $|G| \to \infty$ and $\arg(G) = (1-\sqrt{\gamma})\pi$, thus the image starts at infinity, in the direction determined by the ray $\arg(\cdot) = (1-\sqrt{\gamma})\pi$.

(d) $s = Re^{-i\theta}$, $-\pi/2 \le \theta \le 0$, with $R \gg 1$. This portion maps into the origin of the $G-$plane, because one takes $R \to \infty$ to make the curve surround the whole right-half plane (see [5]).

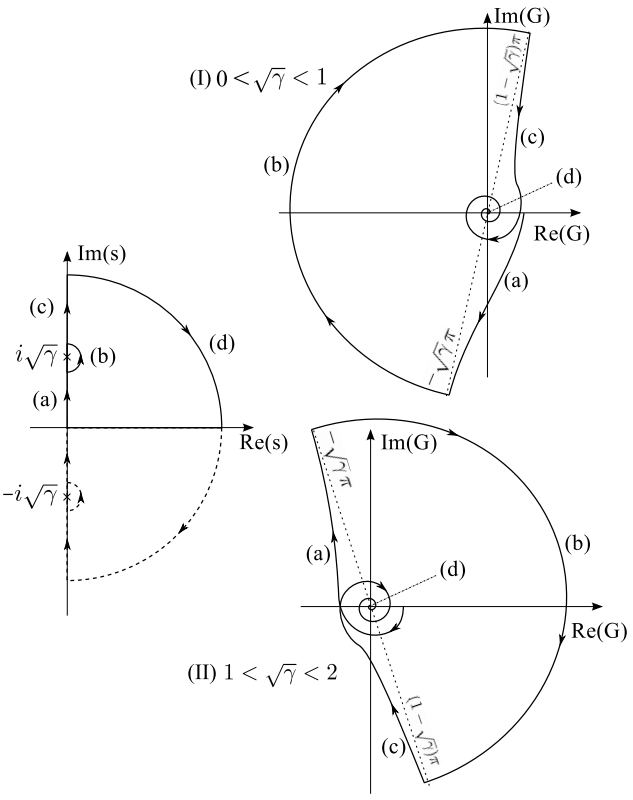

Figure 1: Left: Nyquist contour. Right: Qualitative image of the contour under the function $G(s)$ for $\tau = \pi$, with $0 < \sqrt{\gamma} < 1$ (I) and with $1 < \sqrt{\gamma} < 2$ (II). Only the image for $\mathrm{Im}(s) \ge 0$ is shown in both cases.

From the above analysis, it can be seen that *the equilibrium point y_1^* is stable if the locus of $G(i\omega)$ does not enclose the point $1/\alpha$*. Moreover, the situation is qualitatively different if $2n < \sqrt{\gamma} < 2n+1$, $n \in \mathbb{N} \cup \{0\}$ or if $2n-1 < \sqrt{\gamma} < 2n$, $n \in \mathbb{N}$.

The stability condition/s (SC) can be found by looking at the intersection of $G(i\omega)$ with the real axis. Since

$$G(i\omega) = \frac{e^{-i\omega\pi}}{\gamma - \omega^2} = \frac{\cos\omega\pi}{\gamma-\omega^2} - i\frac{\sin\omega\pi}{\gamma-\omega^2}, \tag{6}$$

it follows that $\mathrm{Im}(G) = 0$ implies $\omega_k = k$, $k \in \mathbb{Z}$, and

$$\mathrm{Re}(G(i\omega_k)) = \frac{(-1)^k}{\gamma - k^2}. \tag{7}$$

Then:

- If $2n < \sqrt{\gamma} < 2n+1$, (as in Fig. 1(I) with $0 < \sqrt{\gamma} < 1$), the curve encloses completely the negative real axis, and y_1^* can be stable only if the point $1/\alpha$ lies on the positive real axis, i.e., $\alpha > 0$. For the part **(a)** of the curve, the intersection with the real axis with greater modulus occurs when $k = 2n$. The SC then reads $\mathrm{Re}(G(i\omega_{2n})) < 1/\alpha$, which using (7) gives
$$\frac{1}{\gamma - (2n)^2} < \frac{1}{\alpha} \Rightarrow \alpha < \gamma - (2n)^2.$$
On the other hand, for the part **(c)** of the Nyquist diagram, the intersection with the real axis with greater modulus is observed when $k = 2n+1$. This produces the following SC:
$$\frac{-1}{\gamma - (2n+1)^2} < \frac{1}{\alpha} \Rightarrow \alpha < (2n+1)^2 - \gamma.$$
The above SC can be understood easily by taking into account Fig. 2(a), where a detail of the Nyquist diagram with $\gamma = 20.5$ ($4 < \sqrt{\gamma} < 5$) is shown. For this particular value of γ, the intersections corresponding to $k = 4$ and $k = 5$ coincide, but it does not happen in general.

- If $2n-1 < \sqrt{\gamma} < 2n$, (as in Fig. 1(II) for $1 < \sqrt{\gamma} < 2$), the curve encloses completely the positive real axis, and y_1^* can be stable only if the point $1/\alpha$ lies on the negative real axis, i.e., $\alpha < 0$. For the part **(a)** of the curve, the intersection with the (negative) real axis with greater modulus occurs when $k = 2n-1$. The corresponding SC is $\mathrm{Re}(G(i\omega_{2n-1})) > 1/\alpha$, which from (7) yields
$$\frac{-1}{\gamma - (2n-1)^2} > \frac{1}{\alpha} \Rightarrow \alpha > (2n-1)^2 - \gamma.$$
For the part **(c)** of the curve, the intersection with the real axis with greater modulus occurs when $k = 2n$. The SC results
$$\frac{1}{\gamma - (2n)^2} > \frac{1}{\alpha} \Rightarrow \alpha > \gamma - (2n)^2.$$
Figure 2(b) shows a detail of the Nyquist diagram with $\gamma = 30.5$ ($5 < \sqrt{\gamma} < 6$), which illustrates the above outcomes.

3.1.1. Generic τ values

The previous results obtained with $\tau = \pi$ can be generalized, now considering τ as a free parameter.

$$G(i\omega) = \frac{e^{-i\omega\tau}}{s^2+\gamma} = \frac{\cos\omega\tau}{\gamma-\omega^2} - i\frac{\sin\omega\tau}{\gamma-\omega^2}. \tag{8}$$

Setting $\mathrm{Im}(G) = 0$, one has $\omega = \omega_k = k\pi/\tau$, $k \in \mathbb{Z}$, but only nonnegative values of k are of effective interest. Thus,

$$\mathrm{Re}(G(i\omega_k)) = \frac{(-1)^k}{\gamma-(k\pi/\tau)^2}, \tag{9}$$

and the asymptotes of the Nyquist diagram are the rays

$$\begin{cases} -\sqrt{\gamma}\tau, & \text{when } \omega \to \sqrt{\gamma}^- \\ -\sqrt{\gamma}\tau+\pi, & \text{when } \omega \to \sqrt{\gamma}^+, \end{cases} \tag{10}$$

for any $\gamma > 0$. For example, if $-\pi < -\sqrt{\gamma}\tau < 0$, $(0 < \gamma < (\pi/\tau)^2)$ the corresponding Nyquist diagram will be similar as the one on Fig. 1(I), i.e., it will enclose the whole negative real axis. On the other hand, if $-2\pi < -\sqrt{\gamma}\tau < -\pi$, $((\pi/\tau)^2 < \gamma < (2\pi/\tau)^2)$ the diagram will surround the whole positive real axis, as in Fig. 1(II).

The general SC for $y_1^* = 0$ will now be deduced following the same reasoning as for $\tau = \pi$.

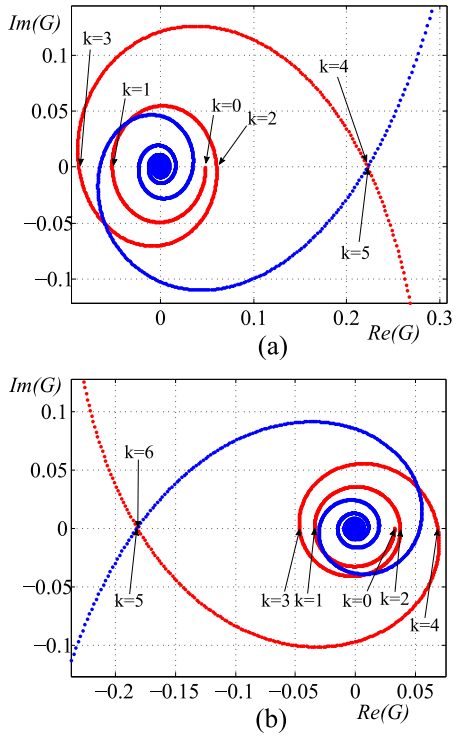

Figure 2: Detail of the Nyquist diagram of $G(s)$ with $\tau = \pi$ and: (a) $\gamma = 20.5$ $(4 < \sqrt{\gamma} < 5)$; (b) $\gamma = 30.5$ $(5 < \sqrt{\gamma} < 6)$. Red (blue) line corresponds to frequencies satisfying $\omega < \sqrt{\gamma}$ $(\omega > \sqrt{\gamma})$. The intersections corresponding to $k = 4$ and $k = 5$ in (a) ($k = 5$ and $k = 6$ in (b)) coincide for these particular γ values, giving possible Hopf-Hopf bifurcations (see Section 4).

- If $(2n\pi/\tau)^2 < \gamma < ((2n+1)\pi/\tau)^2$: The situation is as in Fig. 1(I). A trivial SC is given by $\alpha > 0$. The intersection with greater frequency corresponding to part **(a)** of the diagram (where the modulus is increasing), occurs with $k = 2n$, and the one with lower frequency corresponding to part **(c)** (where the modulus is decreasing), occurs with $k = 2n+1$. One only needs to analyze these two values of k. With $k = 2n$, the SC is given by $\mathrm{Re}(G(i\omega_{2n})) < 1/\alpha$, which using (9) results

  $$\alpha < \gamma - (2n)^2(\pi/\tau)^2.$$

  For $k = 2n+1$, the SC is $\mathrm{Re}(G(i\omega_{2n+1})) < 1/\alpha$, thus from (9) it follows that

  $$\alpha < (2n+1)^2(\pi/\tau)^2 - \gamma.$$

- If $((2n-1)\pi/\tau)^2 < \gamma < (2n\pi/\tau)^2$: The situation is as in Fig. 1(II). A trivial SC is given by $\alpha < 0$. The intersection with greater frequency corresponding to part **(a)** of the diagram, occurs with $k = 2n-1$, and the one with lower frequency corresponding to part **(c)** is observed with $k = 2n$. With $k = 2n-1$, the SC becomes $\mathrm{Re}(G(i\omega_{2n-1})) > 1/\alpha$, which gives

  $$\alpha > (2n-1)^2(\pi/\tau)^2 - \gamma.$$

  And the last SC is $\mathrm{Re}(G(i\omega_{2n})) > 1/\alpha$, which gives

  $$\alpha > \gamma - (2n)^2(\pi/\tau)^2.$$

Table 1 summarizes the SC for the equilibrium point y_1^*.

Table 1: Stability conditions for y_1^* with $r = \pi/\tau$.

Values of γ	SC for y_1^*
$(2n)^2r^2 < \gamma < (2n+1)^2r^2$	$\alpha > 0$; $\alpha < \gamma - (2n)^2r^2$ $\alpha < -\gamma + (2n+1)^2r^2$
$(2n-1)^2r^2 < \gamma < (2n)^2r^2$	$\alpha < 0$; $\alpha > \gamma - (2n)^2r^2$ $\alpha > -\gamma + (2n-1)^2r^2$

3.2. Nontrivial equilibrium point

In the case of y_2^*, from (3), the characteristic function becomes

$$\lambda_2(s) = G(s)J_2 = \frac{(\alpha-2\gamma)e^{-s\tau}}{s^2+\gamma}, \tag{11}$$

and the critical stability condition $\lambda_2(i\omega) = -1$ can be expressed as $G(i\omega) = 1/(2\gamma-\alpha)$. Then, the number of turns of the Nyquist diagram of $G(i\omega)$ around the critical point $1/(2\gamma-\alpha)$ will be determined, for a generic τ value. Using (8) and (9), one can deduce the following:

- If $(2n\pi/\tau)^2 < \gamma < ((2n+1)\pi/\tau)^2$: The situation is like in Fig. 1(I). A trivial SC is given by $2\gamma - \alpha > 0$, or equivalently, $\alpha < 2\gamma$. It is only is necessary to analyze the values of $k = 2n$ and $k = 2n+1$. With $k = 2n$, the SC is given by $\mathrm{Re}(G(i\omega_{2n})) < 1/(2\gamma-\alpha)$, which results in $\alpha > \gamma + (2n)^2(\pi/\tau)^2$.

  With $k = 2n+1$, one gets the SC given by $\mathrm{Re}(G(i\omega_{2n+1})) < 1/(2\gamma-\alpha)$, which yields $\alpha > 3\gamma - (2n+1)^2(\pi/\tau)^2$.

- If $((2n-1)\pi/\tau)^2 < \gamma < (2n\pi/\tau)^2$: The situation is as shown in Fig. 1(II). A trivial SC is given by $2\gamma-\alpha < 0$, i.e., $\alpha > 2\gamma$. It is only is necessary to analyze the cases of $k = 2n-1$ and $k = 2n$.

  With $k = 2n-1$, the SC is $\mathrm{Re}(G(i\omega_{2n-1})) > 1/(2\gamma-\alpha)$, which yields $\alpha < 3\gamma - (2n-1)^2(\pi/\tau)^2$.

  With $k = 2n$ the SC becomes $\mathrm{Re}(G(i\omega_{2n})) > 1/(2\gamma - \alpha)$, namely $\alpha < \gamma + (2n)^2(\pi/\tau)^2$.

Table 2 summarizes the SC for the equilibrium point y_2^*.

Table 2: General SC for y_2^* with $r = \pi/\tau$.

Values of γ	SC for y_2^*
$(2n)^2r^2 < \gamma < (2n+1)^2r^2$	$\alpha < 2\gamma, \quad \alpha > \gamma + (2n)^2r^2$ $\alpha > 3\gamma - (2n+1)^2r^2$
$(2n-1)^2r^2 < \gamma < (2n)^2r^2$	$\alpha > 2\gamma, \quad \alpha < \gamma + (2n)^2r^2$ $\alpha < 3\gamma - (2n-1)^2r^2$

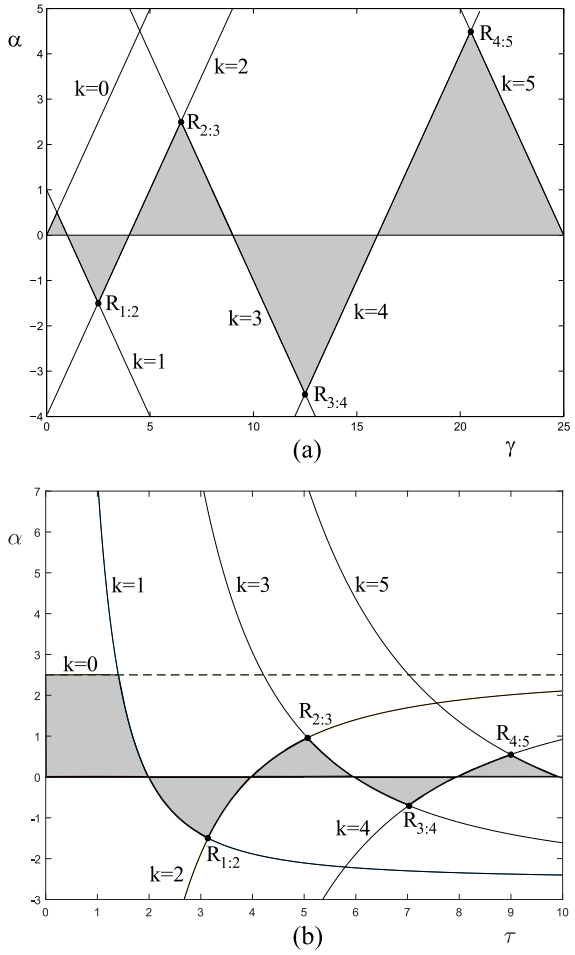

Figure 3: Hopf bifurcation curves and stability regions (shaded) of the equilibrium point y_1^* in (a): $\gamma - \alpha$ plane with $\tau = \pi$ and (b): $\tau - \alpha$ plane with $\gamma = 5/2$. Multiple resonant Hopf-Hopf bifurcation points can be observed.

4. Resonant Hopf-Hopf bifurcations

Consider the equilibrium point y_1^* and its corresponding characteristic function $\lambda_1(s)$ given in (4). The critical stability condition $\lambda_1(i\omega) = -1$ actually represents Hopf bifurcation points if $\omega \neq 0$. From (8) and (9), letting $G(i\omega) = 1/\alpha$, it is simple to obtain explicitly the Hopf bifurcation points as

$$\alpha_k = (-1)^k \left[\gamma - (k\pi/\tau)^2\right], \tag{12}$$

where the point-wise frequency is $\omega = k\pi/\tau$. The above expression, represents straight lines on the $\gamma - \alpha$ plane and hyperbolas on the $\tau - \alpha$ plane, delimiting the stability regions shown in Fig. 3. Moreover, the intersections between some Hopf bifurcation curves lead to resonant Hopf-Hopf bifurcation points, as shown in Fig. 3. It is enough to consider an even value k_1 ($k_1 \neq 0$) and an odd value k_2 in (12) to obtain a resonant Hopf-Hopf point. At a Hopf-Hopf bifurcation point (noted as $\mathrm{R}_{1:2}$, $\mathrm{R}_{2:3}$, etc., in Fig. 3), one obtains Nyquist diagrams as shown in Fig. 2, where two stability boundaries are reached simultaneously.

In addition, if $k_1 = 0$ and k_2 is odd in (12), it generates a zero-Hopf bifurcation point. Particularly, the $1:2$ resonance (noted as $\mathrm{R}_{1:2}$ in Fig. 3) obtained with $\gamma = 5/2$ and $\tau = \pi$ was studied in detail in [1, 2].

5. Conclusions

In this work, a generalized four-parameters version of the model originally proposed in [1] is analyzed. It is found that the system exhibits infinitely many resonant Hopf-Hopf bifurcation points, as well as zero-Hopf points. These results were checked independently using classical techniques for the stability analysis of quasipolynomials.

In a previous work [2], both local and global analysis were performed, in a neighborhood of a $1:2$ resonant Hopf-Hopf point, for the particular case with $\gamma = 5/2$ and $\tau = \pi$. The global analysis of the four parameters model is left for future work.

6. Acknowledgements

This work was supported by UNRN (PI 40/A389), UNS (PGI 24/K064), ANPCyT (PICT 2014-2161) and CONICET (PIP 112-201201-00144).

References

[1] Campbell, S. A. and V. G. LeBlanc, "Resonant Hopf-Hopf interactions in delay differential equations", *SIAM Journal of Dyn. and Diff. Equations*, 10(2), 327-346 (1998).

[2] Gentile, F. S., G. R. Itovich and J. L. Moiola, "Resonant 1:2 double Hopf bifurcation in an oscillator with delayed feedback," *Nonlinear Dynamics*, 91(3), 1779-1789 (2018).

[3] Mees, A. I. and L. O. Chua, "The Hopf bifurcation theorem and its applications to nonlinear oscillations in circuits and systems," *IEEE Trans. Circ. Syst.*, 4, 235-254 (1979).

[4] Moiola, J. L. and G. Chen, *Hopf Bifurcation Analysis: A Frequency Domain Approach*. World Scientific Publishing Co, Singapore (1996).

[5] Ogata, K., *Modern Control Engineering*, Prentice Hall (5th edition), Boston (2010).